Polymer−Solid Interfaces: Influence of Sticker Groups on Structure and Strength†

Liezhong Gong,‡ Anthony D. Friend,§ and Richard P. Wool*,‡,||

Department of Chemical Engineering, University of Delaware, Newark, Delaware 19716, Center for Composite Materials, University of Delaware, Newark, Delaware 19716, and Department of Material Science and Engineering, University of Illinois, 1304 W. Green Street, Urbana, Ill 61801

Received October 28, 1997; Revised Manuscript Received March 17, 1998

ABSTRACT: A model polymer−solid interface, aluminum- (Al-) carboxylated polybutadiene (cPBD), was designed to investigate the influence of the sticker group (−COOH) on the fracture energy (G_{IC}). A model polymer, cPBD, was synthesized through high-pressure carboxylation of polybutadiene (PBD) and contained −COOH randomly distributed along the length of the polymer chains. T-peel tests were used to evaluate the interfacial fracture energy. The effect of the concentration of the sticker groups (ϕ) on the fracture energy was examined, and a critical concentration (ϕ_c), around 3 mol %, was found to give a maximum bonding strength, which was an order of magnitude stronger than the same interface without sticker groups. The fracture energy of Al−cPBD−Al interfaces increased over a range of 10−1000 min annealing time, t, which is much longer than the characteristic relaxation time of PBD at room temperature. The fastest adhesion occurred for sticker group concentrations at ϕ_c, whereas chains with sticker groups at $\phi_c \pm 1\%$ required much longer surface rearrangement times. The dynamics of adhesion was found to be comparable to time-dependent surfaces restructuring, using dynamic contact angle studies. Many of these results could be understood from a self-consistent lattice model developed by Theodorou, which we used to investigate how the sticker groups affect the structure of the interfacial chains. Sticker groups were found to have a strong tendency to segregate to the solid surface, resulting in a large concentration gradient near the solid surface. This phenomenon, together with the extremely slow surface restructuring process of cPBD chains, which relax like tethered chains, partially accounts for the long time dependence of the fracture energy of Al−cPBD−Al interfaces. Modeling also showed that the chain shape and the chain connectivity close to the solid surface was modified. With increasing concentration of sticker groups, the flatness of the chains near the solid substrate decreased at first and then increased, indicating an optimum concentration for efficient chain connectivity within the interfaces. These modeling results predicted a critical concentration of sticker groups for optimum bonding in the sense of cohesive strength, agreeing well with experimental results.

1. Introduction

In recent years, polymer−solid interfaces have become an area of increasing interest both from a fundamental point of view and for practical reasons.[1−3] Applications of such interfaces are widespread in fields such as aerospace, aircraft, automotive, microelectronics, and the food packaging industry, etc. While different properties are of interest for various applications, good adhesion at interfaces is an issue of fundamental importance since it determines the serviceability and reliability of the materials. An interface can meet its desired functional or mechanical purpose only if the interface is strong enough to withstand all stresses and strains that might appear in a practical operation. Formation of an interface that is mechanically weaker will result in a material with poor properties and a shorter service life. The strength of adhesion is determined by the adhesive and cohesive strength of the substrate and the polymer. The addition to polymer chains of sticker groups, which can interact with the solid surface strongly by forming hydrogen, covalent, or ionic bonds, is an efficient and widely used strategy to modify the adhesive strength. A specific application of this method in industry is the improvement of the adhesion properties of polyolefins either by functionalizing the surface chains through different treatments,[4−7] such as corona discharge, high-temperature oxidation, flame treatments, and chromic acid etching, or by using copolymers containing polar functional groups. The cohesive strength of the polymer depends on the density and the primary and secondary structure of the materials, i.e., the conformation and organization of the individual polymer chains and the degree of crystallinity within the interphase.

In general, solid surfaces modify the density distribution of the interfacial chains.[8−11] The structures of polymer chains at the interphase do not necessarily mirror those in the bulk. Introducing sticker groups on polymer chains will result in a specific energetic driving force for the interfacial chains. Therefore, we expect the interplay between the specific energetic driving force and the entropic constraint imposed by the impenetrable solid surface to cause the structure and dynamics of the interfacial chains to have some unique features, which might affect the adhesion strongly. A quantitative understanding of these features is quite desirable and is one of the main goals of this paper.

From a fundamental point of view, the fracture energy of a polymer−solid interface depends on such molecular details as the areal density of the chains (Σ) and the length of the chains (N). Recently, carefully designed experiments have been conducted to explore these types

* To whom correspondence should be addressed.
† Abstract presented to American Physical Society, Kansas City, MO, March 1997.
‡ Department of Chemical Engineering, University of Delaware.
§ University of Illinois.
|| Center for Composite Materials, University of Delaware.

S0024-9297(97)01594-5 CCC: $15.00
Published on Web 05/08/1998

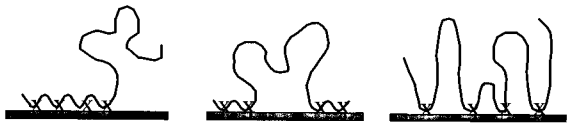

A B C

Figure 1. Three possible distributions of sticker groups along polymer chains and the corresponding interfacial structures.

of molecular details extensively by examining: (1) immiscible polymer−polymer interfaces containing diblock or random copolymer additives,[12−15] (2) polymer−solid interfaces with end tethered polymer chains.[16−18] For a specific interface such as a polymer−solid interface with sticker groups along polymer chains, besides the areal chain density (Σ), and the chain length (N), additional key factors include the concentration of the sticker groups (ϕ), the type of sticker groups, and the distribution of these sticker groups along the polymer chains. The type of sticker groups determines the interaction strength between the polymer and the solid substrate (χ_{P-S}), while the distribution of these sticker groups along the chains controls the sequence structure. As illustrated in Figure 1, generally there are three possible distributions of sticker groups which result in different sequences for linear chains: (A) sticker groups located at one end of the chain, (B) sticker groups on both ends of the chain, and (C) sticker groups distributed through the whole length of the chain. The sequence structures have significant impact on adhesion because they dominate the interfacial structure. For sequence structure (A), the interfacial structure will be similar to that formed by end-grafted polymer chains. The tails of polymer chains will tend to be grafted on the solid surface for sequence structure (B), while a multiloops structure with tails will be anticipated for sequence structure (C). When the sequence distribution along polymer chains is specified, the fracture energy G_{IC} can be expressed as the following fundamental equation:

$$dG_{IC} = \left(\frac{\partial G_{IC}}{\partial \Sigma}\right)_{N,\theta,\chi_{P-S}} d\Sigma + \left(\frac{\partial G_{IC}}{\partial \varphi}\right)_{N,\Sigma,\chi_{P-S}} d\phi + \left(\frac{\partial G_{IC}}{\partial N}\right)_{\Sigma,\phi,\chi_{P-S}} dN + \left(\frac{\partial G_{IC}}{\partial \chi_{P-S}}\right)_{N,\phi,\chi\Sigma} \sum d\chi_{P-S} \quad (1)$$

In this paper, we mainly explore the second term of eq 1, namely the influence of the concentration of sticker groups, by studying a model polymer−solid interface system, in which the sticker groups are distributed through the whole length of the chains (Figure 1C).

A model system, Al−polybutadiene (PBD) interface, was employed in order to eliminate the influence of other complicated factors such as crystallinity, corrosion, etc. Through a carboxylation reaction, carboxylic acid groups (COOH) were introduced onto the backbone of the PBD chains. These groups act as sticker groups because of their ability to interact strongly with an Al (Al_2O_3) surface. The advantage of using the carboxylation reaction over other methods, such as copolymerization, is that it will not change the degree of polymerization of PBD. The peel test was used to evaluate the fracture energy of Al−PBD−Al interfaces as a function of the concentration of the carboxylic acid groups and annealing time (t). In addition, a self-consistent field (SCF) modeling study was used to examine how the addition of the sticker groups impacts the interfacial structure, including the spatial distribution of the sticker groups and shape of the chains.

Scheme 1. Synthesis of Carboxylated Polybutadiene by High-Pressure Carboxylation Reaction

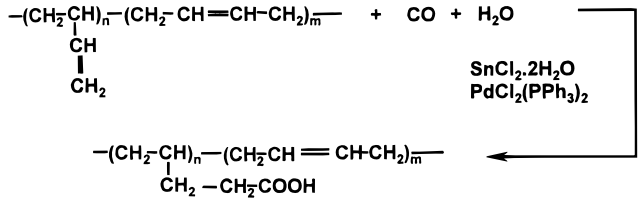

2. Experimental Section

2.1. Synthesis of the Model Polymer. The model polymer, carboxylated polybutadiene (cPBD), was synthesized through high-pressure carboxylation of polybutadiene (PBD), as described in Scheme 1. The procedures are briefly summarized below, and further details can be found elsewhere.[19,20] High molecular weight PBD (trade name Diene 35 AC10) was supplied by Firestone Rubber & Latex Company. The molecular weight and microstructure information are $M_n = 98\,000$, $M_w = 182\,000$, and 10 mol % vinyl (1,2-addition) groups. The catalyst, dichlorobis(triphenylphosphine)palladium ($PdCl_2(PPh_3)_2$), was prepared by following the method described in the literature.[21] In a typical reaction, a solution of PBD (1.08 g), $PdCl_2(PPh_3)_2$ (0.146 g), $SnCl_2 \cdot 2H_2O$ (0.45 g), and H_2O (1.8 mL) in 100 mL of tetrahydrofuran (THF) was transferred to a Parr mini-300 stainless steel reactor. The reactor was pressurized at room temperature to 500 psi with CO and then released. This was done three times, after which the reactor was filled with CO to 1350 psi. The reactor was heated to 145 °C, increasing the pressure to around 1850 psi while the reaction was stirred with a magnetic plate. The reaction times of 4−24 h were used in order to obtain the desired extent of PBD carboxylation. The discharge of the reactor revealed a finely dispersed solution containing palladium black, which was removed by centrifugation at 4000 rpm for 90 min. The polymer products were recovered from the solution by precipitation from a 100 mL mixture of solvent composed of methanol (80 mL), acetone (20 mL), and 5 drops of concentrated hydro chloric acid.

2.2. Characterization of cPBD Samples. The degree of carboxylation of cPBD samples was determined via FTIR. The IR spectra of cPBD solutions in tetrahydrofuran (THF) with known concentrations (∼1.0 mol %) were obtained, and the net absorbances, of the carbonyl groups (∼1730 cm^{-1}) were compared with a calibration curve to get the absolute concentration of COOH. The calibration curve was constructed by using PBD diacid (Aldrich $M_n = 4200$) solution with various concentrations in THF. All spectra were recorded on a Mattson Genesis Fourier transform infrared spectrometer at 4 cm^{-1} resolution and 64 scans. It was found that the concentration of carboxylic acid for the synthesized samples was in the range 0−10 mol %.

Thermal analysis of the synthesized cPBD samples was conducted by using a Du Pont 990 differential scanning calorimeter under N_2 purge at a temperature rate of 10 °C/min. It was found that all cPBD samples did not show a melting point (T_m) and a glass transition above room temperature. This information confirms that all samples synthesized are noncrystalline and are at the rubber state.

^{13}C NMR analysis showed that the carboxylic acid groups were mainly introduced onto the terminal carbon atom of the pendant double bonds of PBD. This result is consistent with others' reports on the carboxylation of low molecular weight PBD.[22]

2.3. Determination of the Interfacial Fracture Energy. The fracture energy, G_{IC}, of the cPBD-Al interfaces was evaluated by a T-peel test as illustrated in Figure 2. The aluminum foil was obtained from Shop-Aid Inc. with a

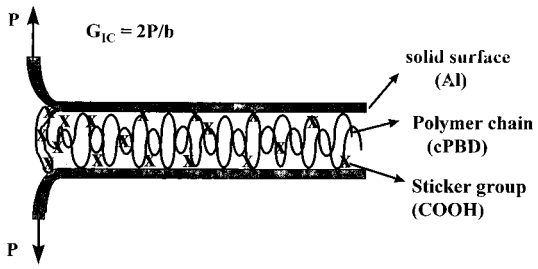

Figure 2. Schematic representation of the peel test.

thickness of 25 μm. Its average roughness of approximately 0.5 μm was determined by a Scanning White Light Interferometer (SWLI). The Al foil was first pretreated overnight at 300 °C in an oven to ensure the formation of a stable layer of native oxide. A layer of cPBD was uniformly cast onto it from 1 wt % solution of toluene. The thickness of the layer of cPBD was estimated to be 15 μm based on the volume of solution cast and the surface area covered. After the toluene was evaporated under vacuum for 15 min, another pretreated Al foil was then put on the top of the cPBD layer to form an Al−cPBD−Al sandwich structure. After being pressed together for 5 min to ensure good contact, the Al−cPBD−Al samples were annealed under 4 kPa of pressure at room temperature for different times and then cut into specimens with dimensions of 60 mm in length and 10 mm in width. The peel tests were conducted on a Mini-44 Instron tensile machine at a cross-head speed of 30 mm/min. The fracture energy, G_{IC}, was obtained from the average of three tests per material and is given by

$$G_{IC} = \frac{2P}{b} \tag{2}$$

where P is the peel load and b is the width of the test sample.

2.3. Dynamic Contact Angle Measurements. Dynamic contact angles of water on cPBD surfaces were measured using the Wilhelmy plate technique. Cover glass slides (Fisher, 24 mm × 50 mm × 1 mm) were immersed in a Nochromix−sulfuric acid solution for 24 h, rinsed extensively with purified water (Fisher HPLC grade), and then dried overnight in a vacuum oven at 100 °C. The clean glass slides were dipped in dilute cPBD−toluene solution (1 wt %) for 24 h and then dried in air and under vacuum for 30 min and 1 h, respectively. The advancing and receding contact angles of cPBD-coated coverslips were measured by using a CAHN dynamic contact angle analyzer at a plate-moving speed of 22 μm/s.

3. Results and Discussion

3.1. Effect of Sticker Groups Concentration on Fracture Energy. The fracture energy of the interfaces, G_{IC}, is plotted vs the concentration of sticker groups (ϕ) in Figure 3. The introduction of a few percent sticker groups onto PBD chains resulted in substantial improvement of the fracture energy of the Al−cPBD−Al assembly. For example, 0.5 mol % of sticker groups on PBD chains led to a 2−3-fold increase in the interfacial adhesion. With the sticker groups increasing to 2.7 mol %, the adhesion strength reached ~300 J/m^2, which is almost an order of magnitude higher than that without sticker groups. However, the fracture energy declined with further increase of the concentration of sticker groups. It is rather surprising to find that an optimal concentration (ϕ_c) of the sticker groups existed for the best adhesion although this ϕ_c was relatively small.

In the literature, others also reported maximum adhesions existed at specific concentrations by examining the influence of the compositions of copolymers on bonding strength. Schultz et al.,[23] studied the modification of the adhesion of polypropylene to aluminum by adding a small quantity of maleic anhydride grafted polypropylene. It was found that, with the introduction of maleic anhydride grafted polypropylene, the peel strength first increased and then decreased as a result of the formation of a weak boundary layer. This boundary layer was found to be made of the low molecular weight grafted chains, which were formed during the grafting reactions.

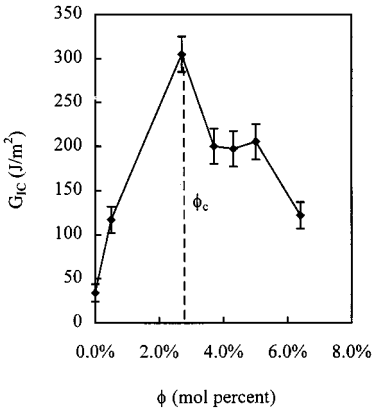

Figure 3. Influence of the concentration of sticker groups on the fracture energy of Al−cPBD−Al interfaces (annealing time = 1000 min, room temperature).

Mao and Reegen[24] investigated the peel strength between a pigmented epoxy ester resin substrate and the copolymers of methyl methacrylate and acrylamide as a function of the concentration of acrylamide in the copolymer. They found that the peel strength of the copolymer increased continuously up to 10 mol % of acryamide and then decreased with further increasing of the acryamide. They attributed this phenomenon to the increase in the crystallinity of the copolymer with further introduction of acryamide. Even earlier, Mclaren and Seiler[25] evaluated the adhesion strength of vinyl chloride−vinyl acetate−maleic acid copolymers to aluminum and found that maximum adhesion occurred at 1.6 mol % of maleic acid. They believed that the fall off in adhesion of the copolymer containing more than 1.6 mol % of maleic acid was due to excessive corrosion of the substrate, i.e., aluminum. However, all the above explanations cannot be used to interpret the results in the present work. There was no reason to expect that, at 145 °C, a PBD chain scission reaction would occur and produce lower-molecular-weight cPBD during the carboxylation reactions, which would form a weak boundary layer as reported by Schultz et al.[23] Thermal analysis showed that PBD and cPBD did not degrade below 240 °C under N_2. Additional experiments were carried out to confirm that there was no degradation of PBD in the reaction environment. A PBD−THF solution without H_2O was subjected to 145 °C and 2000 psi for 24 h. This PBD was then dissolved in toluene and the intrinsic viscosity was determined by a Ubbelohde viscometer. It was found that the intrinsic viscosity remained identical before and after the treatment, indicating that there was no PBD chain scission. Thermal analysis also showed that all the cPBD samples used were rubberlike and did not possess a melting temperature, suggesting no influence of crystallinity. Additionally, after examining the fracture surfaces of the Al−cPBD−Al assemblies, we did not observe any corrosion on the aluminum.

We suspect that a critical concentration results from the variation of the secondary structure and molecular

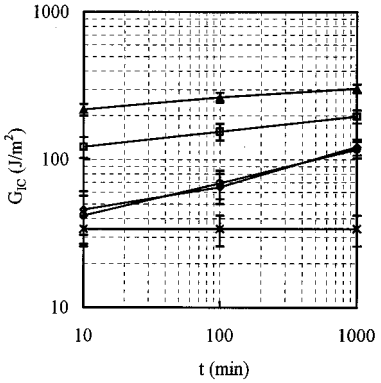

Figure 4. The log−log plot of G_{IC} vs t over a time range of 10−1000 min, showing $G_{IC} \approx G_0 t^m$ (−COOH mol %: 0.0% (cross), 0.5% (circle), 2.7% (triangle), 4.3% (square), and 6.4% (diamond)).

connectivity (i.e., the orientation and conformation) of the polymers within the interface. The fracture energy of Al−cPBD−Al interfaces is limited by the weaker of the adhesive strength and the cohesive strength. When the amount of sticker groups is low (less than ϕ_c), the limiting factor is the adhesive strength. With increasing sticker group concentration, the adhesive strength between cPBD at the near-surface layer and the solid substrate is improved. However, at concentrations greater than ϕ_c, the cohesive strength of cPBD between the near-surface and the far-surface layer may be reduced due to the dense attachment of the near-surface layer to the solid substrate. As a result, the cohesive strength could even be lower than the adhesive strength and the interface might fail cohesively instead of adhesively, leading to a weaker adhesion. During the peel test, we did observe that the failure mode of all the Al−cPBD−Al interfaces tested was cohesive, while the failure mode of Al−PBD−Al interfaces ($\phi = 0\%$) was adhesive. The possibility of the formation of weaker cohesive strength was also discussed by Gutman, Chakraborty, and Shaffer,[8−10] who speculated the possibility of cohesive failure through the near-surface layer based on their theoretical results about polymer chain adsorption from a dilute or semidilute solution. Experimental evidence showing this possibility has been reported recently by Beck Tan et al.,[26] who investigated the reactive reinforcement of the interfaces of sulfonated polystyrene/poly (2-vinylpyridine). Their findings were that 5−7 mol % sulfonation gave rise to an optimum interfacial fracture toughness. The decline in toughness with further increasing of the sulfonation was partially attributed to the excessive interfacial grafting density, which caused the interfacial chains to entangle with themselves rather than with the chains in the bulk.

3.2. The Effect of Bonding Time on the Fracture Energy. The annealing-time dependence of the fracture energy of Al−cPBD−Al interfaces is shown in Figure 4. It can be seen that G_{IC} for the samples made from uncarboxylated PBD had no annealing-time dependence, while the fracture energy of Al−cPBD−Al interfaces showed a strong time dependence in the experimental time scale of 10−1000 min. The fracture energy went to a plateau with further annealing to 2000 min. The time-dependent set in Figure 4 can be described by $G_{IC} \sim G_0 t^m$, where G_0 is defined as the initial fracture energy ($t = 10$ min) of the interface. It seems that both G_0 and m are a function of the concentration of the carboxylic acid groups. As shown

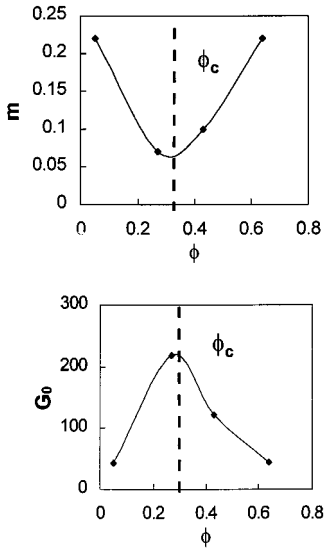

Figure 5. Dependence of the values of m and G_0 on the concentration of sticker groups (results based on the mean values of G_{IC} from Figure 4).

in Figure 5, when the concentration is close to the critical concentration, i.e., when $\phi = 2.7$ mol %, G_0 was high but m was small, indicating that the interface gained most of the adhesion strength rapidly. When the concentration is deviated from the critical one, i.e., when $\phi = 0.5$ or 6.5 mol %, G_0 was lower but m was larger, suggesting that interfacial bonding developed slowly.

The development of the adhesion strength of a polymer−solid interface involves the establishment of interfacial contact at the molecular level through wetting and the formation of physical and/or chemical interactions.[1,27] In our case, since all polymers were rubberlike, full wetting contact between polymers and solid surfaces was ensured before annealing by pressing together the sandwich structure of the samples. The interactions between the polymers and Al surfaces were possibly van der Waals and hydrogen bonding. The time dependence of adhesion can be compared with the characteristic relaxation time of polymer chains, which can be calculated by

$$\tau_r = \frac{R_g^2}{2D} \tag{3}$$

where R_g and D are the radius of gyration and the self-diffusion coefficient of the polymer chains, respectively.

According to Roland and Bohm,[28] the self-diffusion coefficient of PBD with $M_n = 84\,780$ and $M_w = 93\,258$ is $D = 3.4 \times 10^{-13}$ cm^2/s at 23 °C. Since $D \sim M^{-2}$, for our case at room temperature, the characteristic relaxation of PBD is around 20 s, which is several orders of magnitude smaller than the corresponding experimental time scale in Figure 4. Thus, the development of adhesion strength involves relaxation processes, which are considerably longer than the bulk polymer relaxation time.

During the formation of the Al−cPBD−Al interfaces, COOH groups have to diffuse and adsorb to the solid surface because of the energetic driving force resulting from the specific and strong interaction between −COOH and the Al_2O_3 surface. Once a COOH group from a chain is adsorbed to the solid surface, the whole chain is trapped and can be approximated as a tethered chain

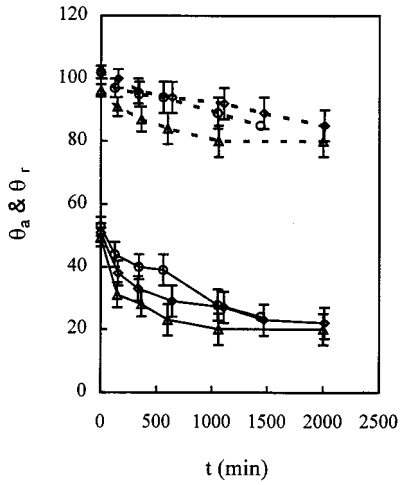

Figure 6. Dynamic contact angles of cPBD samples vs water-annealing time (dashed line, advancing; solid line, receding). Symbols are the same as those in Figure 4).

with two free ends. It has been shown that tethered chains relax to equilibration through retraction of the free ends similar to the diffusion process of star polymers, which could be very slow.[13,29−31] The situation could be even worse if two sticker groups from the same chain were adsorbed. Without breaking the bonding sites, the segments between the two attachment sites could only penetrate into the rest of the chains by making "excursions".[31] Therefore, the restructuring time of cPBD chains within the interfaces will be much longer than that in the bulk. The long relaxation time of the partially tethered cPBD chains at the interfaces could account for the experimental results that revealed a long time dependence of the fracture energy (Figure 4). In addition, we suspect the restructuring process could be related to the specific structure that cPBD chains adopt within the interfaces. The structure of interfacial chains is a specific function of the concentration of sticker groups, which we will explore later.

3.3. Surface Rearrangement Dynamics. The surface restructuring process resulting from the diffusion and adsorption of COOH groups to the hydrophilic solid substrate was further examined by dynamic contact angle analysis. The cPBD-coated glass cover slides were immersed in water, and the dynamic contact angles (θ) of cPBD-coated surfaces were determined vs aging time. Since the hydrophilic COOH groups have a specific interaction with water through formation of hydrogen bond, there is a driving force for them to move to the surface and reorient. Consequently, the hydrophilic surface should exhibit and lead to decreasing contact angles of cPBD with increasing water-contact time. Figure 6 shows the results of the advancing and receding contact angles of cPBD in terms of contact time with water. It can be seen that both advancing and receding angles decreased, indicating the reconstruction of the surface. Another significant feature is that the advancing angle changed from hydrophobic (>90°) to hydrophilic (<90°) after being immersed in water for a certain length of time. The appreciably large hysteresis between the advancing and receding angles is mainly due to the surface heterogeneity. A similar surface restructuring phenomenon was also observed by others[32,33] for plasma treated PE, PP, PET, and PC surfaces.

After normalizing the advancing and receding angles of Figure 6 with respect to initial values, some interesting features become apparent. As illustrated in Figure 7, we can argue that the concentration of COOH had an influence on the surface restructuring process. For example, the contact angles of the samples with $\phi = 0.5$ and 6.4 mol % show a longer time dependence than those for cPBD with $\phi = 2.7$ mol %. This result is qualitatively consistent with what was observed from the peel tests and provides additional support to the argument that the surface restructuring depends on the concentration of the sticker groups. We will explore the details of the polymer−solid interface structure in the next section.

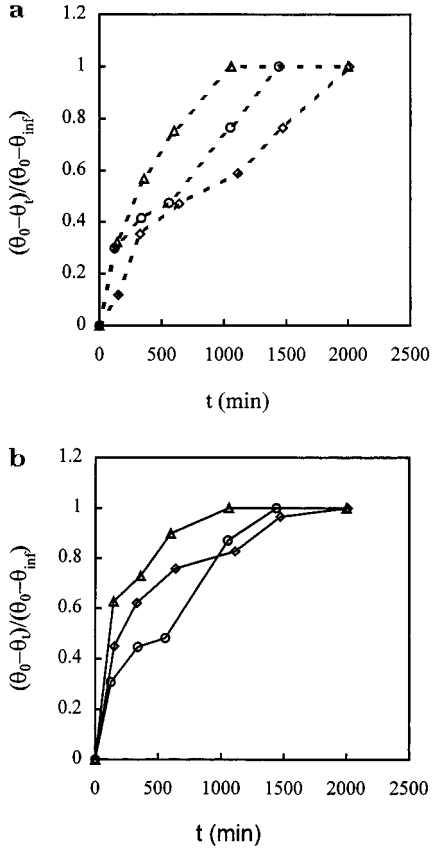

Figure 7. (a) Normalized advancing angles vs annealing time (θ_0, mean angle before annealing; θ_t, mean angle at annealing time t; θ_{inf}, mean angle at the end of the experiment). −COOH concentrations are the same as those in Figure 4. (b) Normalized receding angles vs annealing time.

3.4. Self-Consistent Field Modeling Study. 3.4.1. The SCF Model. We suspect the adhesion of polymer−solid interfaces is determined by the adsorption of the sticker groups at the solid surface as well as the long range connectivity of the interfacial chains with the polymer matrix. These concepts were explored by employing a modeling study to investigate how sticker groups modify the structure of polymers at the polymer−solid interface. As illustrated in Figure 8, the Al−cPBD−Al interface was modeled as a polymer melt between two parallel solid walls, which are molecularly smooth. These walls are separated by a distance of $2d$ in the z direction and are infinite in the x and y directions. The cPBD chain was represented by a random copolymer composed of two types of units, A and B, which were the same size. The unit A has a strong interaction with the solid walls and represents the sticker group (COOH). The B units have a weaker interaction with the walls and represent the PBD units without sticker groups. We are particularly interested

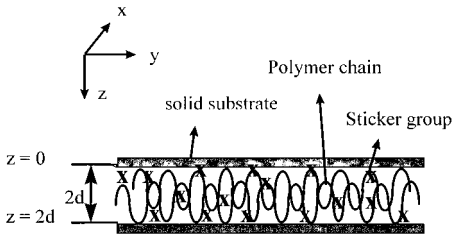

Figure 8. System used to model Al−cPBD−Al interfaces (*x*, *y* directions are infinite).

in (1) the spatial distribution of sticker groups at the interface, and (2) how the structure of the chains is related to the concentration of the sticker groups (ϕ_{A-bulk}). In this work a self-consistent field lattice model (SCFLM) developed by Theodorou[34−37] was used. The SCFLM was used because it has been shown to be efficient in simulating the structure of sharp interfaces such as random copolymer melt−solid interfaces.[37] In addition, it is able to give salient features such as the chain shape, the monomer spatial distribution and the bond orientation within the interfaces.[38]

The SCFLM used is essentially an extension of Flory−Huggins thermodynamics to anisotropic melts[38] and is briefly summarized as follows. The space constrained between two solid walls, as shown by Figure 8, is modeled as being composed of lattices, the sites of which can be occupied by the units of polymer chains. There are $2d$ lattice layers between the two walls and d is assumed to be large enough that the conformational characteristics in the neighborhood of layer d (the middle of the interface) are the same as those of the bulk copolymer. The constrained polymer is considered to be a monodisperse linear random copolymer, consisting of two types of segments, A and B, and having degree of polymerization, N. By defining the unconstrained bulk polymer as a reference state, the partition function (Q) of the interfacial lattice system, for a given set $\{n_c\}$ of conformations, can be expressed as the product of an entropic term and an energetic term

$$Q[d,N,T,\{n_c\}] = \left(\frac{\Omega}{\Omega^*}\right)e^{-U/RT} \qquad (4)$$

where Ω is defined as the number of ways to arrange the set of conformations $\{n_c\}$ on the lattice interfacial system, Ω^* represents the number of ways to arrange the same chains on the lattice in the bulk polymer; U is the difference of the potential energy between the interfacial system and a system of the same chains in the unconstrained bulk.

Flory's procedure of laying the chains onto the lattice one by one was used to evaluate the entropic term in the above expression. Through a mean-field approximation, the potential energy, U, was obtained by enumerating the interacting segment pairs in both the interfacial system and the bulk polymer. A set of coupled and closed nonlinear algebraic equations can be obtained by imposition of the equilibrium condition as well as by consideration of the self-consistency requirements relating the conformational distribution of chains to the density distribution of polymer segments. Solving the equations, one could obtain structure as a function of layer number.

The computation was carried out by using polymer modeling software from Biosym/Molecular Simulations.[39] To conduct the calculations, the INTERPHASES module applied to random copolymer/solid interphases was used. This module simulated a random copolymer in a cubic lattice. The degree of polymerization, N, of 80 was chosen for all the results reported. A value of $N = 200$ was also tried for several runs of calculation and the general features were found to be consistent in general. The interphase between the solid surfaces consisted of 40 lattice layers ($2d = 40$). Since the B−surface and A−B interactions are weak, their interaction parameters χ_{B-S} and χ_{A-B} (similar to the standard Flory−Huggins interaction parameter) were both assigned low values of 0.1. Under these conditions, the influence of the A−surface interaction, χ_{A-S}, and the concentration of A groups, ϕ_{A-bulk}, on the interfacial chain structure was examined. To reduce the influence of the quenched disorder carried by the random polymer chains, the results were averaged through several individual realizations of the computation on a specific sticker group concentration and chain length. It is believed that averaging over a couple of individual realizations of SCF calculation will be able to reduce the influence resulting from the quenched disorder.[40]

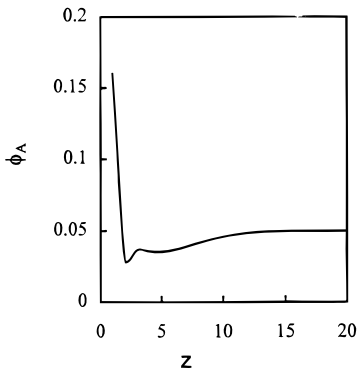

Figure 9. Spatial distribution of sticker groups within interphases, predicted from the SCFLM ($\phi_{A-bulk} = 5.0$ mol %; $\chi_{A-S} = 2.5$, $N = 80$).

3.4.2. The Spatial Distribution of the Sticker Groups. Figure 9 illustrates the spatial distribution of sticker group A at the interfaces with $\chi_{A-S} = 2.5$ and $\phi_{A-bulk} = 5$ mol %. It is found that the concentration of sticker groups on the solid surface layer (ϕ_{A-1}) is over three times higher than that in the bulk due to the selective adsorption of the sticker groups. The depletion of A segments on the second lattice layer is observed. This is because the second layer must accommodate the B units as a result of chain connectivity. On the subsequent layers, the concentration of A unit increases gradually and reaches the bulk value eventually. This general feature is consistent with that reported by Theodorou (Figure 13 in ref 37). However, the enrichment of A on the solid surface was more significant in this study due to the far stronger interaction between segment A and the surface. In addition, this strong interaction disturbs the distribution of the sticker groups to a distance of three to four times the unperturbed chain radius of gyration.

The influence of sticker-group interaction strength (χ_{A-S}) on their segregation at the interface was further explored. As shown in Figure 10, with increasing χ_{A-S}, the concentration of A on the solid surface (ϕ_s) increased up to four times ϕ_{bulk}. However full occupancy on the solid substrate is not reached. This result implies that a substantial number of A groups needs to diffuse to the surface during the formation of the interface. This leads to a large concentration gradient at the layers

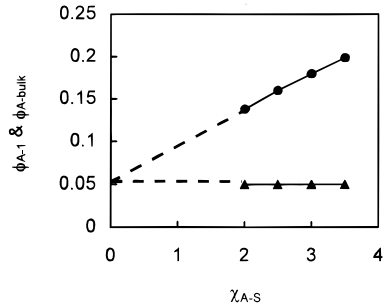

Figure 10. Influence of χ_{A-S} on the surface enrichment of sticker groups, predicted from SCFLM ($\phi_{A-bulk} = 5.0$ mol %, $N = 80$) (filled triangle, bulk concentration; filled circle, surface concentration).

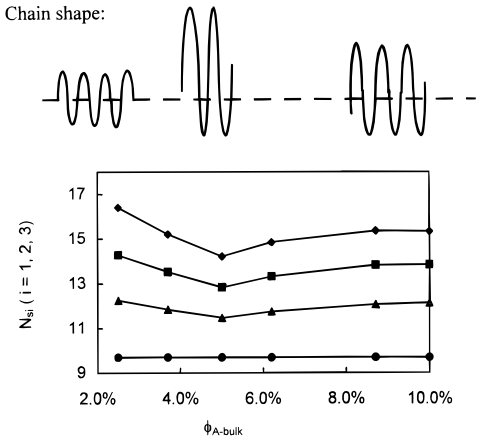

Figure 11. Impact of the concentration of sticker groups on the shape of the interfacial chains, predicted from SCFLM ($\chi_{A-S} = 2.5$, N = 80) (filled diamond, $i = 1$; filled square, $i = 2$; filled triangle, $i = 3$; filled circle, $i =$ bulk).

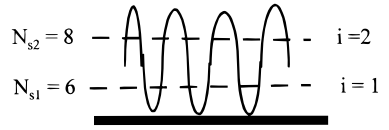

Figure 12. Pictorial representation of N_{si}, the average number of segments per chain at layer i.

closest to the solid surface. The phenomenon is probably one of the reasons why the fracture energy of Al−cPBD−Al interfaces was discovered to be strongly time dependent. Extrapolating the data in Figure 10 to $\chi_{A-s} = 0$ (sticker group has the same interaction strength to the substrate as the backbone unit), we can see that ϕ_s reaches ϕ_{bulk}, indicating no segregation of sticker groups.

3.4.3. The Influence of the Concentration of Sticker Groups on the Chain Shape. The influence of the concentration of the sticker groups (ϕ_{A-bulk}) on the chain shape is shown in Figure 11. The ordinate N_{si} is the average number of segments per chain at layer i and is a sensitive measure of the local structure. The physical meaning of N_{si} can be easily understood in the following way. If a chain is modeled as being composed of many loops in two dimensions and we cut the loops by a straight line parallel to the solid surface, then N_{si} represents the number of points at which the line hits the loops as illustrated in Figure 12. A high value of N_{si} corresponds to flat chains in the layer (highly adsorbed with many contacts), while a low value of N_{si} indicates that polymer chains are elongated (brushlike, few contacts) in a direction perpendicular to the substrate surface.

In a polymer bulk, N_{s-bulk} should be scaled as the square root of the chain length because of the random walk chains. When the chain length, N, is in the range from 10 to 500, Theodorou found that N_{s-bulk} is correlated perfectly with N by the equation[34]

$$N_{s-bulk} = 1.0854N^{1/2} \tag{5}$$

At $N = 80$, based on the above equation, N_{s-bulk} should be 9.7, which is exactly what we obtained. When neutral chains (chains without sticker groups) are arranged within the interphase, N_{s1} should be bigger than N_{s-bulk} due to the entropic constraint imposed by the impenetrable solid substrate. For neutral chains with $N \rightarrow \infty$, N_{s1} should be around $2N_{s-bulk}$ as the result of the imposition of the impenetrable boundary condition.

From Figure 11, we can see that, when ϕ_{A-bulk} is in the range 2−10 mol %, N_{si} is larger than the value in the bulk, indicating that polymer chains prefer to lie flat on the couple of layers close to the solid surface. This result coincides with other reports.[41] However, a significant feature is that, as ϕ_{A-bulk} increases from 2 to 10 mol % (χ_{AS} held constant), N_{si} decreases and then increases past a minimum. The structure of the near polymer−solid interface and the longer range connectivity of the surface chains with the bulk entanglement network above the surface are both affected in an interactive way. This type of relation between N_{si} and ϕ_{A-bulk} results from the balance of the energy gain and the entropy loss as a consequence of the selective adsorption of the sticker groups onto the solid substrate. The specific interaction between sticker groups and the solid substrate provides a driving force for sticker groups to move to the solid surface. At the same time, this interaction leads those segments without sticker groups to stretch away from the solid substrate, consequently causing an entropic penalty to the whole interfacial system. The chain shapes corresponding to the value of N_{si} are illustrated in the top part of Figure 11. The lowest N_{si} indicates that, at this critical concentration ϕ_c, the chains form fewer numbers of loops and extend far away from the solid surfaces. Therefore, they are able to entangle with other chains more efficiently and increase their connectivity with other chains. The implication of these results to an adhesion problem is that an optimum composition exists for cohesive strength. With further increase of ϕ, the interface might fail cohesively due to the less efficient entanglement in the near surface layers. This type of behavior is exactly as what has been seen in Figure 3. Additionally, we did find that the failure mode was cohesive for all Al−cPBD−Al interfaces. Since the degree of polymerization of PBD used was 1810, which was much higher than the value of 80 used in the simulation, the absolute values of the variation of N_{si} with −COOH for cPBD would become very large. The big change of N_{si} would be enough to account for the considerable change of fracture energy of Al−cPBD−Al interfaces with the concentration of −COOH. Furthermore, when a real interface like Al−cPBD−Al is concerned, the influence of χ_{A-S} on N_{si} should be taken into account. If we assume the interaction at the interfaces is mainly due to hydrogen bonding with a typical value of enthalpy around 3.5 kcal/mol,[42] then χ_{A-S} is around 6 at room temperature, which differs from the value of 2.5, as used in Figure 11.

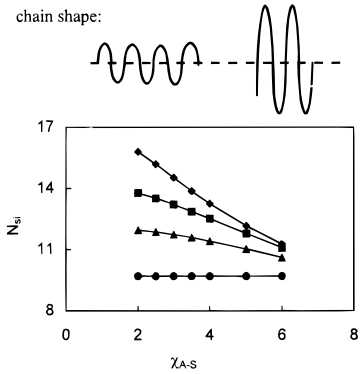

Figure 13. Influence of χ_{A-S} on the interfacial chain shape at a constant bulk concentration of sticker groups (ϕ_{A-bulk} = 3.0 mol %, N = 80), predicted from SCFLM (filled diamond; i = 1; filled square, i = 2; filled triangle, i = 3; filled circle, i = bulk).

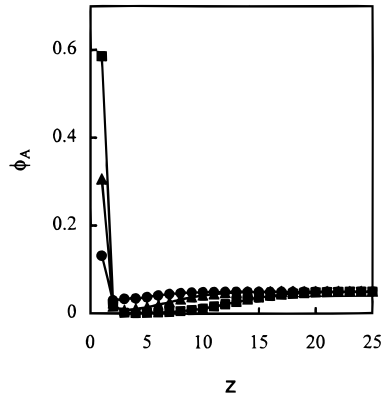

Figure 14. Spatial distribution of sticker groups within interphases for three typical sequence distributions of sticker groups in Figure 1 (N = 100, ϕ_{A-bulk} = 5.0 mol %) (filled square, sequence A; filled triangle, sequence B; filled circle, sequence C).

The influence of χ_{A-S} on interfacial chain shape is shown in Figure 13. As χ_{A-S} increases (ϕ_{A-bulk} held constant) from 2 to 6, N_{si} decreases monotonically although it is still greater than N_{s-bulk}. The phenomenon results from the larger energetic gain with higher values of χ_{A-S} so that polymer chains at the interface can stretch farther away from the solid substrate. It suggests that different sticker groups will lead to different interfacial chain structures.

3.4.4. The Influence of Sequence Distributions on Interfacial Structure. As pointed out previously, the sequence structure of sticker groups is another key factor to control adhesion at polymer−solid interfaces. The influence of the three typical sequence structures (Figure 1) on the spatial distribution of sticker groups and the chain shape at interfaces was explored, and the results are shown in Figures 14 and 15. The parameters for computation were kept the same as before except employing N = 100, χ_{A-S} = 2.0, d = 25, and ϕ = 5%. From Figure 14, we can see that sticker groups of sequence A (tails) have the greatest tendency to segregate to the solid substrate, while those of type C (random copolymer) have the least tendency. This is because the entropic penalty corresponding to the segregation of sticker groups is the lowest for sequence A and the highest for sequence C. From Figure 15, it is found that N_{si} at the interface is smaller than N_{s-bulk} for sequence A, indicating that polymer chains lay on the solid surface perpendicularly and have a brushlike

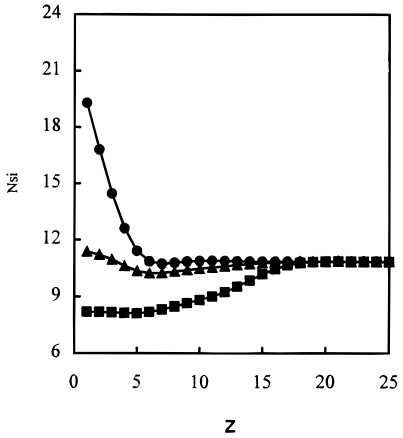

Figure 15. Distribution of N_{si} within interphases for three typical sequence distributions of sticker groups shown in Figure 1 (N = 100, ϕ_{A-bulk} = 5.0 mol %) (filled square, sequence A; filled triangle, sequence B; filled circle, sequence C).

conformation. For sequence B (loops), N_{si} is close to N_{s-bulk}, suggesting the chain shape is not perturbed very much. While polymer chains for sequence C stay on the solid substrate parallel to the surface because N_{si} at the interface is greater than N_{s-bulk}. We expect that the different interface structure resulting from various chain sequence structures will impact adhesion properties significantly. Brushes of high density will have low N_{si} values resulting in poor connectivity and low adhesion. Sequence B requires both ends to be attached to provide strong connectivity, if the loops are long enough. However this may not always be achieved; both ends may not be attached leading to a weak adhesion. For sequence structure C, the balance between the adsorption of sticker groups onto the solid substrate and the high chain connectivity might be easier to attain by selecting the type and the concentration of sticker groups.

4. Conclusions

We have studied the effect of the sticker groups (−COOH) on the fracture energy of Al−cPBD−Al interfaces and found that a small amount of sticker groups was able to improve the fracture energy considerably. The relationship of the concentration of the sticker groups and the interfacial fracture energy was evaluated and a critical concentration (ϕ_c), around 3 mol %, was found to give a maximum bonding strength, which was an order of magnitude higher than that of Al−PBD-Al interfaces. The fracture energy of Al−cPBD−Al interfaces increased over a range of annealing time from 10 to 1000 min, while the relaxation time for PBD at room temperature was only around 20 s. The relationship of G_{IC} and t in the experiment time scale can be modeled as $G_{IC} \approx G_0 t^m$, where the values of G_0 and m were found to be a function of the concentration of the sticker groups. The value of m was small and G_0 was big with ϕ close to ϕ_c, indicating adhesion was formed most rapidly at ϕ_c. With ϕ_c deviating from ϕ_c, m became larger and G_0 became smaller, suggesting that the interfacial bonding developed slowly.

On the basis of a self-consistent lattice model developed by Theodorou, a computer simulation was conducted to investigate how the sticker groups affect the structure of the interfacial chains. It was found that the sticker groups tend to segregate to the solid surface significantly, resulting in a large concentration gradient

of the sticker groups in the lattice layers close to the solid substrate. This behavior, combined with the extremely slow surface restructuring process of cPBD chains, which move like tethered chains, partially accounted for the long time dependence of the fracture energy of Al−cPBD−Al interfaces. Modeling also showed that the chain shape and connectivity close to the solid surface was perturbed by the addition of the sticker groups. The flatness of the chains close to the solid surface decreased with the addition of sticker groups but increased upon reaching an optimum concentration. This optimum concentration signified efficient chain connectivity within the interfaces. The modeling results predicted a critical concentration of sticker groups for the best cohesive strength, which were consistent with the experimental observations.

Acknowledgment. This work was supported by the National Science Foundation through Grant DMR-9596-267 and Hercules Incorporated, Wilmington, Delaware. We would like to thank Dr. Konstantin Goranov for his assistance during the set up of the reactor system.

References and Notes

(1) Wool, R. P. *Polymer Interfaces: Structure and Strength*; Hanser/Gardner: New York, 1995.
(2) de Gennes, P. G. *Soft Interfaces*; Cambridge University Press: Cambridge, England, 1997.
(3) *Polymer/Inorganic Interfaces II*; MRS Symposium; 1995.
(4) Hjertberg, T.; Lakso, J. E. *J. Appl. Polym. Sci.* **1989**, *37*, 1287.
(5) Stralin, A.; Hjertberg, T. *Surf. Interface Anal.* **1993**, *20*, 337.
(6) Liston, E. M.; Martinu, L.; Wertheimer, M. R. *J. Adhesion Sci. Technol.* **1993**, 1091.
(7) Andre, V.; Arefi, F.; Amouroux, J.; Lorang, G. *Surf. Interface Anal.* **1990**, *16*, 241.
(8) Gutman, L.; Chakraborty, A. K. *J. Chem. Phys.* **1994**, *101*, 10074.
(9) Scott Shaffer, J. *Macromolecules* **1995**, *28*, 7447.
(10) Gutman, L.; Chakraborty, A. K. *J. Chem. Phys.* **1995**, *103*, 10733.
(11) Brown, H. R.; Russell, T. P. *Macromolecules* **1996**, *29*, 798.
(12) Creton, C.; Kramer, E. J., Hadiioannou, G. *Macromolecules* **1991**, *24*, 1846.
(13) Brown, H. R. *Macromolecules* **1993**, *26*, 1666.
(14) Kramer, E. J.; Norton, L. J.; Dai, C. A.; Sha, Y.; Hui, C. Y. *Faraday Discuss.* **1994**, *98*, 31.
(15) Reichert, W. F.; Brown, H. R. *Polymer* **1993**, *34*, 2289.
(16) Deruelle, M.; Tirrell, M, Marciano, Y.; Hervet, H.; Leger, Liliane *Faraday Discuss.* **1994**, *98*, 55.
(17) Lin, R.; Wang, H.; Kalika, D. S.; Penn, L. S. *J. Adhesion Sci. Technol.* **1996**, *10*, 327.
(18) Lin, R.; Quirk, R. P.; Kuang, J.; Penn, L. S. *J. Adhesion Sci. Technol.* **1996**, *10*, 341.
(19) Friend, A. D. Master Thesis, University of Illinois at Urbana-Champaign, 1995.
(20) Paper in preparation.
(21) Jenkins, J. M.; Verkade, J. G. *Inorg. Synth.* **1968**, *11*, 108.
(22) Narayanan, P.; Iraqi, A.; Cole-Hamilton, D. J. *J. Mater. Chem.* **1992**, *2*, 1149.
(23) Schultz, J.; Lavielle, L.; Carre, A.; Comien, P. *J. Mater. Sci.* **1989**, *24*, 4363.
(24) Mao, T. J.; Reegen, S. L. in *Adhesion & Cohesion*; Edited by Weiss, P., Ed.; Elsevier Publishing Company, **1962**; p 109.
(25) Mclaren, A. D.; Seiler, C. J. *J. Polym. Sci.* **1949**, *4*, 63.
(26) Beck Tan, N. C.; Peiffer, D. G.; Briber, R. M. *Macromolecules* **1996**, *29*, 4969.
(27) Wu, S. H. *Polymer Interface and Adhesion*; Dekker: New York, 1982.
(28) Roland, C.M.; Bohm, G. G. A. *Macromolecules* **1985**, *18*, 1310.
(29) O'Connor, K.; Mcleish, T. *Faraday Discuss.* **1994**, *98*, 67.
(30) O'Connor, K.; Mcleish, T. *Macromolecules* **1993**, *26*, 7322.
(31) Deutsch, J. M.; Yoon, H. *Macromolecules* **1994**, *27*, 5720.
(32) Morra, M.; Occhiello, E.; Garbassi, F. in *Metallized Plastics 2*; Mittal, K. L., Ed.; Plenum Press: New York, 1991; p 363.
(33) Lavielle, L. In *Polymer Surface Dynamics*; Andrade, J. D., Ed.; Plenum Press: New York, 1988; p 45.
(34) Theodorou, D. N. *Macromolecules* **1988**, *21*, 1400.
(35) Theodorou, D. N. *Macromolecules* **1988**, *21*, 1391.
(36) Theodorou, D. N. *Macromolecules* **1988**, *21*, 1411.
(37) Theodorou, D. N. *Macromolecules* **1988**, *21*, 1422.
(38) Theodorou, D. N In *Physics of Polymer Surfaces and Interfaces*; Sanchez, I. C., Ed.; Butterworth-Heinemann: Oxford, England, 1992; p 139.
(39) BIOSYM/Molecular Simulations manual, Polymer 3.0.0, part 1, **1995**; 6-1.
(40) Gersappe, D.; Fasokla, M.; Israels, R.; Balazs, A. *Macromolecules* **1995**, *28*, 4753.
(41) Wattenbarger, M. R.; Chan, H. S.; Evans, D. F.; Bloomfield, V. A.; Dill, K. A. *J. Chem. Phys.* **1990**, *93*, 8343.
(42) March, J. *Advanced Organic Chemistry*, 4th ed.; John Wiley & Sons: New York, 1992; p 76.

MA9715942